DOI: 10.1002/cmdc.200700003

Structure–Activity Studies on Suramin Analogues as Inhibitors of NAD$^+$-Dependent Histone Deacetylases (Sirtuins)

Johannes Trapp,[a] Rene Meier,[b] Darunee Hongwiset,[c] Matthias U. Kassack,[c] Wolfgang Sippl,[b] and Manfred Jung*[a]

Suramin is a symmetric polyanionic naphthylurea originally used for the treatment of trypanosomiasis and onchocerciasis. Suramin and diverse analogues exhibit a broad range of biological actions in vitro and in vivo, including, among others, antiproliferative and antiviral activity. Suramin derivatives usually target purinergic binding sites. Class III histone deacetylases (sirtuins) are amidohydrolases that require nicotinamide adenine dinucleotide (NAD$^+$) as a cofactor for their catalytic mechanism. Deacetylation of the target proteins leads to a change in conformation and alters the activity of the proteins in question. Suramin was reported to inhibit human sirtuin 1 (SIRT1). We tested a diverse set of suramin analogues to elucidate the inhibition of the NAD$^+$-dependent histone deacetylases SIRT1 and SIRT2 and discovered selective inhibitors of human sirtuins with potency in the two-digit nanomolar range. In addition, the structural requirements for the binding of suramin derivatives to sirtuins were investigated by molecular docking. The recently published X-ray crystal structure of human SIRT5 in complex with suramin and the human SIRT2 structure were used to analyze the interaction mode of the novel suramin derivatives.

Introduction

Histone deacetylases are a group of chromatin-modifying enzymes that cleave acetyl groups from N-terminal lysine residues in histones and other non-histone proteins, modifying the activity of the proteins in question.[1,2] In contrast to histone deacetylase classes 1 and 2, class 3 enzymes, the so-called sirtuins, depend on nicotinamide adenine dinucleotide (NAD$^+$) for their catalytic mechanism. During catalysis, the acetyl moiety of the peptide substrate is transferred to the cosubstrate, and nicotinamide and *O*-acetyl-ADP-ribose are formed as a consequence of the acetyl transfer. Seven members of NAD$^+$-dependent deacetylases have been discovered in humans so far (SIRT1–7) and are classified on the basis of homology to the yeast silent information regulator 2 (Sir2). Sirtuins are implicated in a broad range of biological functions including ageing, cell-cycle regulation, and apoptosis.[3,4]

Only a few inhibitors are available for sirtuins so far: the physiological inhibitor nicotinamide,[5] sirtinol[6] (**1**) and derivatives,[7] and splitomicin,[8] with its related analogues[9] (see Figure 1). Other inhibitors have been discovered with virtual screening approaches.[10,11] Most of these inhibitors display only low inhibitory potency in the micromolar range. Several attempts were made to assess the therapeutic potential of sirtuin inhibitors: HR73 (**2**), a derivative of splitomicin, succeeded in blocking transactivation of retroviral TAT protein by inhibition of SIRT1.[12] Recently, the discovery of indoles as selective SIRT1 inhibitors furnished initial compounds with nanomolar inhibitory potency (for example, compound **3**).[13] Recent research has shown that sirtuin inhibition holds promise for cancer therapy.[14] Of particular interest is the fact that the sirti-

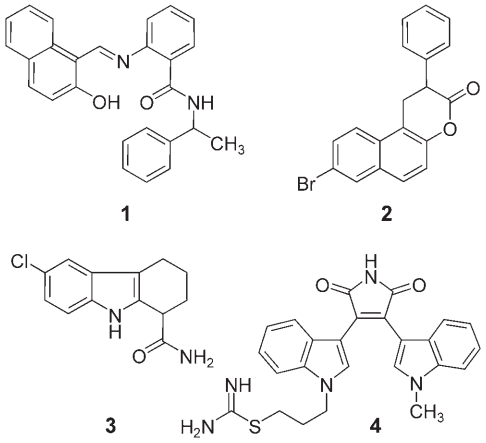

Figure 1. Known sirtuin inhibitors.

[a] *Dr. J. Trapp, Prof. Dr. M. Jung*
Institute of Pharmaceutical Sciences
Albert-Ludwigs-Universität Freiburg
Albertstraße 25, 79104 Freiburg (Germany)
Fax: (+49) 761-203-6321
E-mail: manfred.jung@pharmazie.uni-freiburg.de

[b] *R. Meier, Prof. Dr. W. Sippl*
Department of Pharmaceutical Chemistry
Martin-Luther-Universität Halle-Wittenberg
Wolfgang-Langenbeckstraße 4, 06120 Halle/Saale (Germany)

[c] *D. Hongwiset, Prof. Dr. M. U. Kassack*
Institute of Pharmaceutical and Medicinal Chemistry
Heinrich-Heine-Universität Düsseldorf
Universitätsstraße 1, 40225 Düsseldorf (Germany)

nol analogue cambinol shows anticancer activity in a mouse model.[15] A screen for sirtuin activators revealed suramin (**5a**) and the two related compounds NF023 (**7a**) and NF279 as potent inhibitors of SIRT1 at 100 μM (see Figures 2 and 4 below).[16] Suramin is a symmetric polyanionic naphthylurea originally used for the treatment of trypanosomiasis and onchocerciasis. The lead compound and diverse analogues exhibit a broad range of biological actions in vitro and in vivo, including antiproliferative and antiviral activity, among others.[17] The action of suramin is often ascribed to its ability to interact with purinergic binding sites.[18–20]

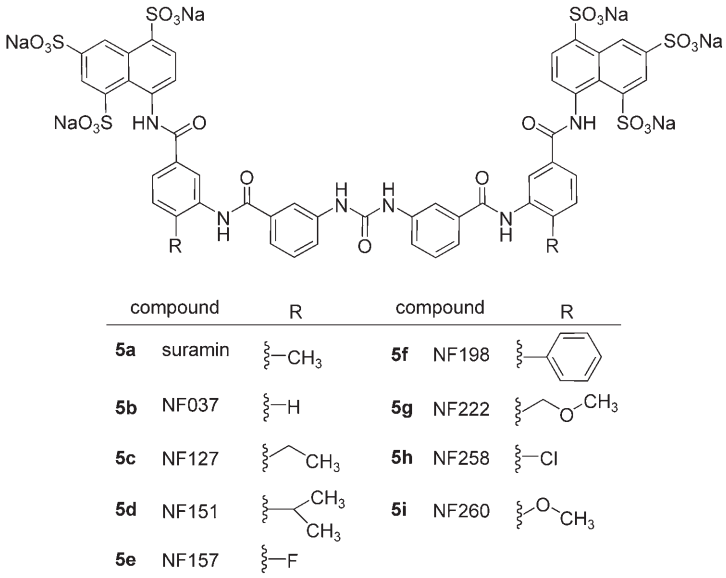

Figure 2. Suramin and related structures.

We were the first to perform a systematic approach to look for mimics of adenosine triphosphate, that is, kinase inhibitors, which can act as sirtuin inhibitors by targeting the adenosine sub-pocket of the NAD^+ binding site. We identified the disubstituted bis(indolyl)maleimide Ro31-8220 (**4**, Figure 1) as a potent selective inhibitor of SIRT2.[21] Thus, adenomimesis is a viable tool to develop new sirtuin inhibitors.

Based on our results with kinase inhibitors and the initial published findings reported for suramin, we decided to perform a systematic structure–activity study for suramin analogues as sirtuin inhibitors. We tested a series of about 30 suramin analogues to obtain structure–activity relationships (SARs) for SIRT1 and 2. Additionally, the structural requirements for the binding of suramin derivatives to sirtuins were investigated by means of molecular docking and analysis of favorable interaction fields. For this purpose we considered the known X-ray crystal structures of human SIRT2 and the structure of the human SIRT5 homologue in complex with suramin that was solved by Schuetz et al.[22] while we were working on the experiments presented herein. Surprisingly, this showed that suramin does not bind to the adenine binding pocket, but to the nicotinamide binding pocket. The suramin derivatives that we have developed represent potent and selective sirtuin inhibitors.

Results and Discussion

Enzyme inhibition

All compounds were evaluated for their ability to inhibit human SIRT1 and 2 in vitro using a fluorescent deacetylase assay. This double enzymatic assay uses ZMAL,[23] an acetylated lysine derivative, as peptide substrate. In an initial step, this substrate is deacetylated by the sirtuin. This deacetylation forms the metabolite (ZML), which is a substrate for trypsin in contrast to the acetylated ZMAL. Thus, in a second step the fluorescent 7-aminomethylcoumarin (AMC) is released from the metabolite by tryptic cleavage which allows quantitation of the enzymatic activity.[24] Human SIRT1 was prepared as an N-terminal GST-tagged protein (GST = glutathione-S-transferase), whereas SIRT2 was produced with an N-terminal His_6 tag.[25]

As mentioned above, suramin (**5a**) and related sulfonated urea derivatives were discovered in 2003 as inhibitors of SIRT1 during a screen for sirtuin activators.[16] The three discovered compounds showed good inhibition of SIRT1 at 100 μM, but further characterization was not reported. We used our assay system to reproduce the inhibition data to establish IC_{50} values, and found suramin to be a potent inhibitor of SIRT1 (IC_{50} = 297 nM) and SIRT2 (IC_{50} = 1150 nM) (Table 1). In subsequent steps, derivatives of the lead compound suramin were assayed against SIRT1 and 2. The first variations concerned the methyl groups on the benzoyl moiety of suramin, which were replaced by small aliphatic groups, halogen atoms, or aromatic residues. Several variations provided inhibitors with increased potency toward both SIRT1 and SIRT2. Most structural variations lead to a slight increase in inhibition (less than twofold for SIRT1 and less than threefold for SIRT2). The best SIRT1 inhibitor is the unsubstituted **5b** (195 nM), and the best SIRT2 inhibitor is the chlorinated compound **5h** (407 nM). Larger substituents such as methoxymethyl in **5g** and phenyl in **5f** rather led to decreased inhibition. Generally, **5a** and most of the closer analogues were unselective or modestly selective for SIRT1, with **5a** showing the best selectivity (about fourfold), whereas **5f** is slightly selective (about twofold) for SIRT2.

We then investigated the effect of structural variations of the suramin core structure. Replacement of the central symmetric bis(*meta*-carboxyphenyl)urea moiety by an isophthalic acid led to an active compound only if the central benzene ring was substituted with an amino group (as in **6c**; see Figure 3). Compound **6c** is the most potent in this study (IC_{50} = 93 nM for SIRT1), and besides compounds such as **3** with similar potency, the most potent sirtuin inhibitor described so far. It is also highly selective for SIRT1 (24-fold over SIRT2).

Further downsizing the center of the molecule to a carbonyl group still produced active compounds **7**, again with a preference for SIRT1. Similar substitution patterns on the *meta*-ami-

Table 1. Inhibition data for SIRT1 and SIRT2.

Compd	Name	SIRT1		SIRT2	
		IC_{50} [nM][a] or Inhibition Data	SE	IC_{50} [nM] or Inhibition Data	SE
1	sirtinol	123451	49694	53011[b]	22517
4	Ro31-8220[b]	3934	556	799	226
5a	suramin	297	10	1150	123
5b	NF037	165	19	585	53
5c	NF127	223	14	612	124
5d	NF151	308	9	449	25
5e	NF157	283	12	467	175
5f	NF198	1713	131	929	55
5g	NF222	662	28	1725	140
5h	NF258	339	11	407	99
5i	NF260	233	12	510	31
6a	NF342	28% at 25 μM		44% at 80 μM	
6b	NF674	43% at 5 μM		31% at 80 μM	
6c	NF675	93	5	2261	674
7a	NF023	236	9	7912	1645
7b	NF150	1286	103	24% at 80 μM	
7c	NF156	284	10	4160	757
7d	NF259	466	46	44% at 80 μM	
7e	NF058	430	137	39522	2937
8a	NF763	56% at 5 μM		65% at 80 μM	
8b	NF770	42% at 25 μM		41% at 80 μM	
9a	NF290	34% at 5 μM		7% at 80 μM	
9b	NF762	53% at 5 μM		17% at 80 μM	
9c	NF769	70% at 25 μM		58% at 80 μM	
10	NF136	581	35	60% at 20 μM	
11	NF444	13% at 50 μM		19% at 80 μM	
12	NF343	35% at 25 μM		45% at 80 μM	
13a	NF443	20% at 50 μM		11% at 80 μM	
13b	NF451	NI[c] at 50 μM		14% at 80 μM	
14a	NF154	525	104	15534	2894
14b	NF155	47% at 5 μM		NI[c] at 80 μM	
15	NF669	53% at 50 μM		56% at 80 μM	
16	AMI-1	32495	2699	53474	3263

[a] Values are means of duplicate experiments ±SE. [b] Data from reference [21]. [c] NI = no inhibition.

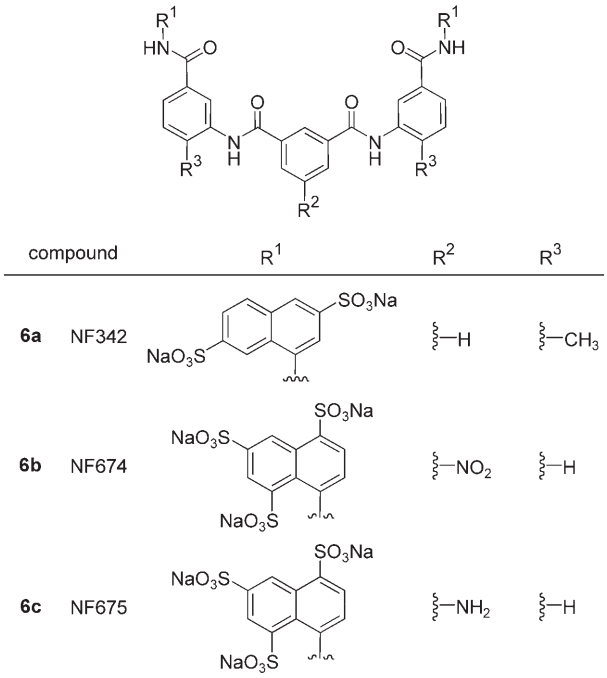

Figure 3. Substituted *meta*-anthranilic acid derivatives.

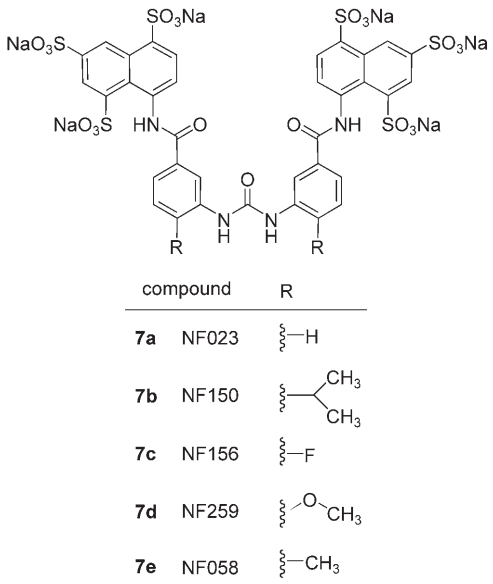

Figure 4. Small ureas.

nobenzoic acid portions as in the suramin analogues **5** were investigated for their effect on enzyme inhibition. The unsubstituted inhibitor **7a** is somewhat more potent toward SIRT1 (236 nM) than suramin (**5a**), but is sevenfold less potent (7.9 μM) than **5a** toward SIRT2. Its fluorinated analogue **7c** is similar to **5a** on SIRT1. Methoxy (compound **7d**) and methyl (compound **7e**) substitution lead to a twofold decrease in IC_{50}, and the larger isopropyl group in **7b** decreased the activity fivefold relative to **5a** and **7a**. All of these compounds have at least 15-fold selectivity for SIRT1 over SIRT2. For **7b** and **7d** we can only estimate the selectivity, which should be at least 180-fold for **7d** with a submicromolar activity on SIRT1 (Figure 4).

Figure 5 shows analogues **8** of suramin (**5a**) and decreased size analogues **9** with modifications of the naphthyl moiety. Removal or substitution of one sulfonyl group by a methoxy substituent again led to a strong decrease in inhibitory potency in relative to suramin. Pronounced rearrangement of the suramin structure, as in derivatives **10**–**13**, leads mostly to weak or inactive compounds, with the notable exception of the biphenyl **10** (581 nM toward SIRT1; see Figure 6). Truncation of one half of the suramin structure decreased inhibition greatly if an amino substituent is present (compound **14b**), but with a nitro group (compound **14a**) potent SIRT1 inhibition (525 nM) is observed (see Figure 6). Figure 6 also presents two more inhibitors (compounds **15** and **16**) with only minor similarity to suramin and weak activity. The binaphthylurea compound AMI-1 (**16**), originally classified as an inhibitor of arginine methyltransferases in vitro and in vivo,[26] also shows some inhibitory activity against SIRT1 and SIRT2. Established sirtuin inhibitors sirtinol (**1**) and **4** were tested as reference compounds.

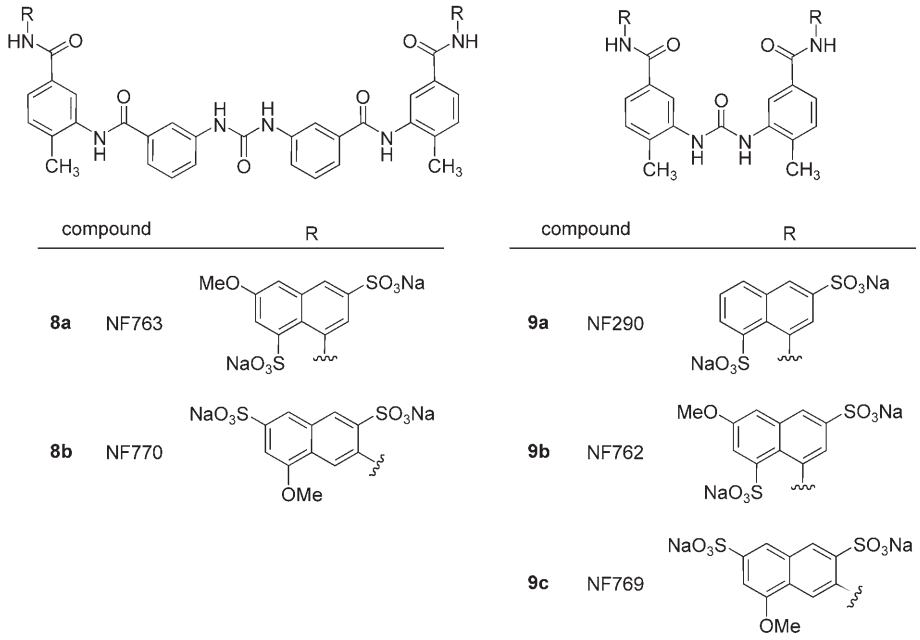

Figure 5. Suramin derivatives and small ureas with variations in the sulfonic acid pattern of the naphthyl scaffold.

Examination of the inhibitor binding site

To determine the structural requirements for binding and inhibiting sirtuins, we analyzed the available crystal structures of sirtuin proteins. The X-ray crystal structures of several Sir2 proteins have been published in the last few years, whereas no 3D structure is available for SIRT1.[27,28] All resolved Sir2 structures contain a conserved catalytic domain of 270 amino acids with variable N and C termini. Consistent with the high sequence similarity in the catalytic domain, the available structural data on the Sir2 proteins also show conservation in the tertiary structure (Figure 7A and B). The structure of the catalytic domain consists of a large classical Rossmann fold and a small zinc binding domain. The acetylated peptide binds in the cleft between the two domains and forms an enzyme–substrate β sheet with two flanking strands from the enzyme. The acetyllysine residue inserts into a conserved hydrophobic pocket, and NAD^+ binds nearby. The interaction of NAD^+ with the residues of the binding pocket can be examined in several sirtuin X-ray structures in which the cofactor has been cocrystallized. Structural comparison of available NAD^+–sirtuin complexes from the Protein Data Bank revealed a highly conserved NAD^+ binding site. In particular, the adenosine binding sub-pocket shows a similar conserved architecture in all known sirtuin structures. In contrast, the nicotinamide binding sub-pocket and the peptide–substrate binding region show larger deviations among the various sirtuin crystal structures.

We have previously described the development of another series of SIRT2 inhibitors[21] including adenosine mimetics such as the bis(indolyl)maleimide Ro31-8220 (**4**), which were originally developed as kinase inhibitors. Based on docking studies that we carried out for human SIRT2 and competition experiments with NAD^+, we found that the compounds interact with the adenine sub-pocket of human sirtuins and not with the substrate pocket where the acetylated lysine residue is bound. Due to the structural dissimilarity between the adenosine mimetics and suramin, it is clear that the suramin derivatives interact in a different way with sirtuin proteins. The different binding sites for suramin, NAD^+, and adenosine mimetics are shown in Figure 7C; a 2D representation is shown in Figure 7D.

A recently published X-ray structure of suramin in complex with the human SIRT5 homologue[22] suggests that the binding site for suramin is between the nicotinamide binding pocket and the cleft for the acetylated peptide, thus inhibiting the deacetylation step. Therefore, despite its known affinity to purinergic binding sites, suramin does not act on the NAD^+ binding pocket of SIRT5.

In a first step of our theoretical study we analyzed the binding mode of suramin by using the published SIRT5 crystal structure (PDB code: 2NYR)[22] and the program GRID. The calculated GRID contour maps were superimposed on the crystal structure of SIRT5 and compared with the position of the cocrystallized suramin molecule and the amino acids of the active site. In the SIRT5 crystal structure the sulfonic acid groups of suramin form four hydrogen bonds with polar amino acid residues (backbone NH of Phe70, Arg71, Tyr102, and Arg105). The location of the sulfonic acid residues agrees well with calculated GRID fields derived with a carboxyl group (Figure 8A). The field obtained with the aromatic GRID is less precisely defined (Figure 8B). In the SIRT5 crystal structure the symmetric suramin molecule interacts with two enzyme monomers by addressing the same binding pockets on the two monomers. Whether this binding mode is an artefact of the crystallization procedure or has a physiological meaning is not yet clear. Subsequently we tested whether the docking program GOLD[29] is able to reproduce the experimentally observed binding mode of suramin. For this purpose we used the dimer of SIRT5 as observed in the crystal structure. The observed low rmsd value between top-ranked docking solution and X-ray structure of 1.3 Å (heavy atoms) showed that GOLD is able to correctly predict the bound conformation of suramin in the dimer of SIRT5 (Figure 9). When only one monomer was used for the docking we could reproduce the interaction of one half of the symmetrical suramin, whereas for the second half no specific interaction domain could be detected (data not shown).

Next, we analyzed the structural differences between the human SIRT5 structure (with bound suramin, PDB code: 2NYR)

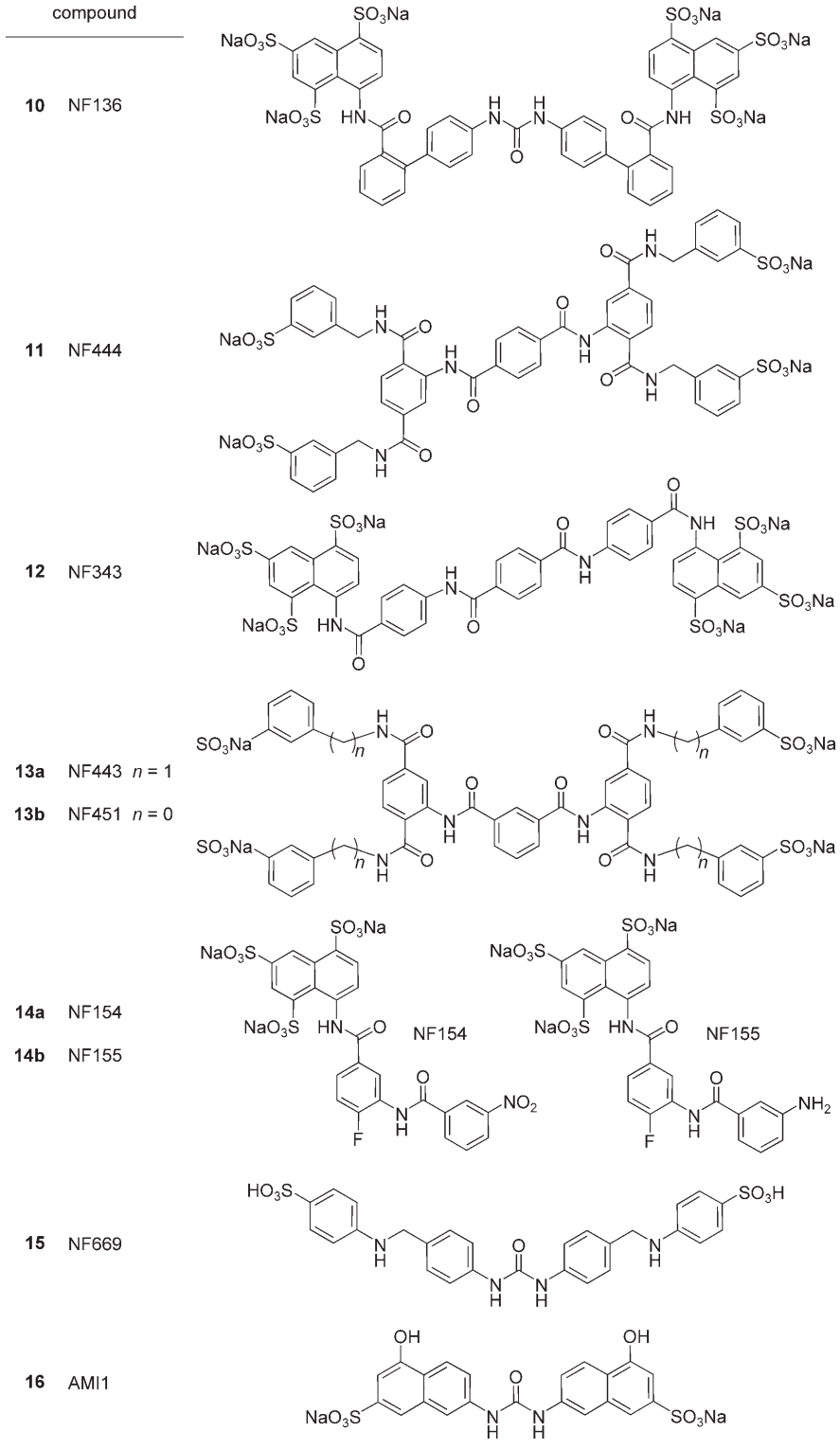

Figure 6. Miscellaneous inhibitors.

and the human SIRT2 structures (PDB code: 1J8F). When both structures were superimposed on their conserved backbone regions (rmsd 2.9 Å) it turned out that the NAD^+ binding pocket is similar, whereas the binding site for suramin shows structural differences in both proteins. Arg 105 and Tyr 102, which interact with the sulfonic acid groups of suramin, are substituted by Leu 138 and Leu 134 in SIRT2, respectively (Figure 10). Arg 97, the homologue of Arg 71 in SIRT5, is oriented toward the adenine binding site in SIRT2 and therefore does not face toward the suggested suramin binding site. Furthermore, the binding pocket of SIRT2 is wider than the narrow pocket observed in the SIRT5 structure. In preliminary docking runs GOLD was not able to produce reasonable docking results for suramin and the synthesized inhibitors. It is known from various Sir2 crystal structures that some parts of the NAD^+ cofactor and the substrate binding pocket are flexible, and thus able to adopt different conformations in complex with different ligands (Figure 7 A and B). Therefore, we modified the SIRT2 binding pocket slightly by adopting the conformation of the corresponding region in SIRT5. The resulting minimized and equilibrated SIRT2 model was subsequently analyzed for favorable interaction regions (Figure 11 A and B). The GRID fields obtained for the SIRT2 model show differences in location and strength compared with SIRT5. The carboxyl probe in particular shows weaker interaction at the SIRT2 binding pocket (Figure 11 A). This is the result of the substitution of two polar residues (Arg 105 and Tyr 102) in the SIRT2 structure by hydrophobic amino acids. However, two favorable interaction regions can still be detected which might explain the binding of the suramin derivatives at SIRT2.

In a subsequent step, the most potent suramin derivatives **5a–5i** were docked into the SIRT2 model (monomer). The docking results show that an interaction of the inhibitors with SIRT2 similar to that of suramin in SIRT5 is possible. The naphthyl ring bearing the three sulfonic acid groups is positioned between Arg 97, Phe 119, and Phe 235 (Figure 12 A). Arg 97, Phe 96, and the backbone NH group of Phe 70 are hydrogen bond donors to the sulfonyl

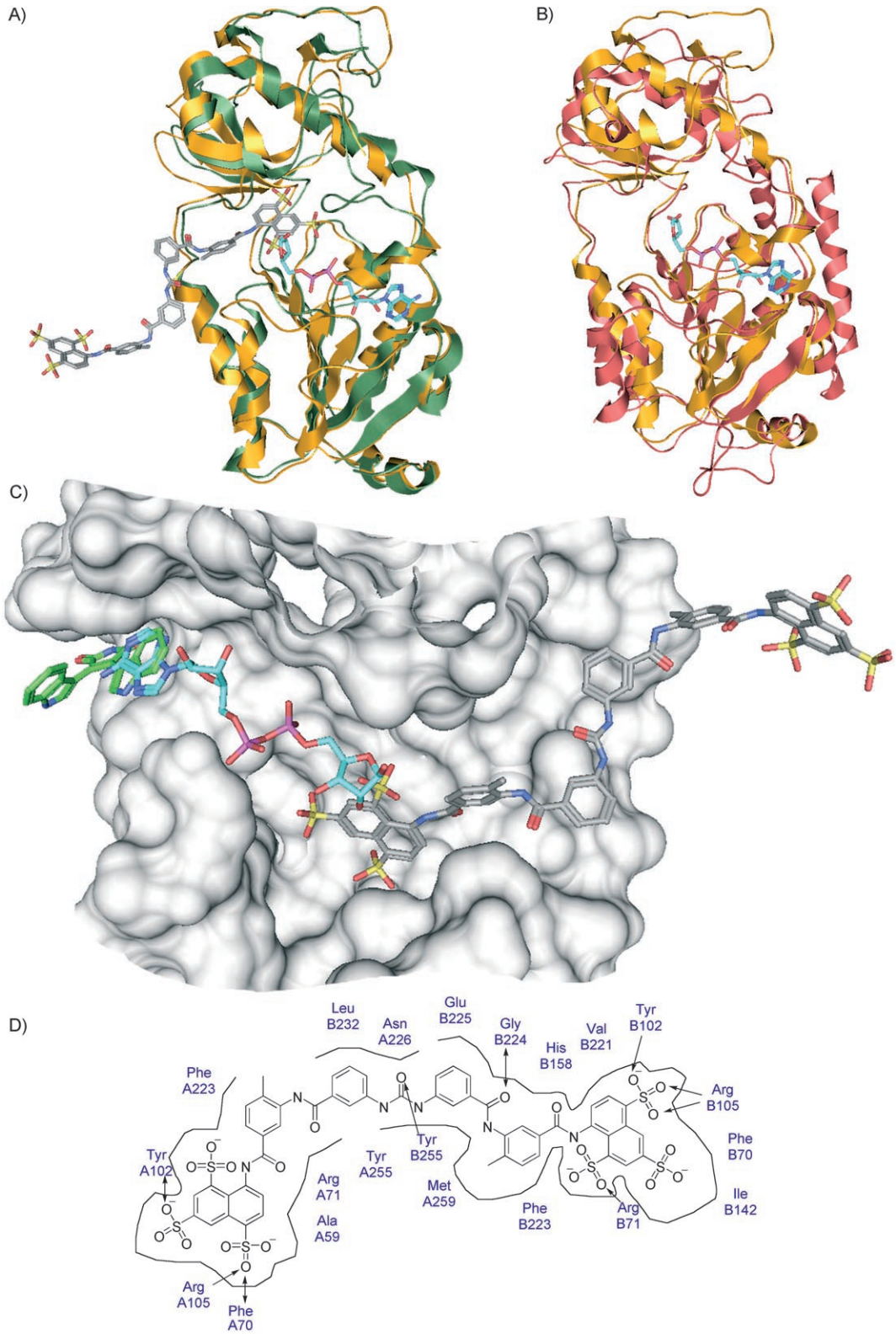

Figure 7. A) Superimposition of the two SIRT5 crystal structures: SIRT5 (PDB code: 2NYR, dark green ribbon) in complex with suramin (atom-type colored) and SIRT5 (PDB code: 2B4Y, orange ribbon) in complex with adenosine-5-diphosphoribose (cyan carbon atoms). B) Superimposition of human SIRT5 crystal structure (PDB code: 2B4Y, orange ribbon) in complex with adenosine-5-diphosphoribose (cyan carbon atoms) and the human SIRT2 structure (PDB code: 1J8F, red ribbon). C) Comparison of the interaction mode of suramin (atom-type coded) and adenosine-5-diphosphoribose (cyan carbon atoms) at SIRT5 with the binding mode of bis(indolyl)maleimide Ro31-8220 (**4**, green carbon atoms) as obtained from previous docking studies.[21] The Connolly surface (calculated with MOE) of the binding pocket is displayed. D) Schematic 2D representation of the interaction between suramin and SIRT5. Hydrogen bonds between inhibitor and enzyme are marked by arrows.

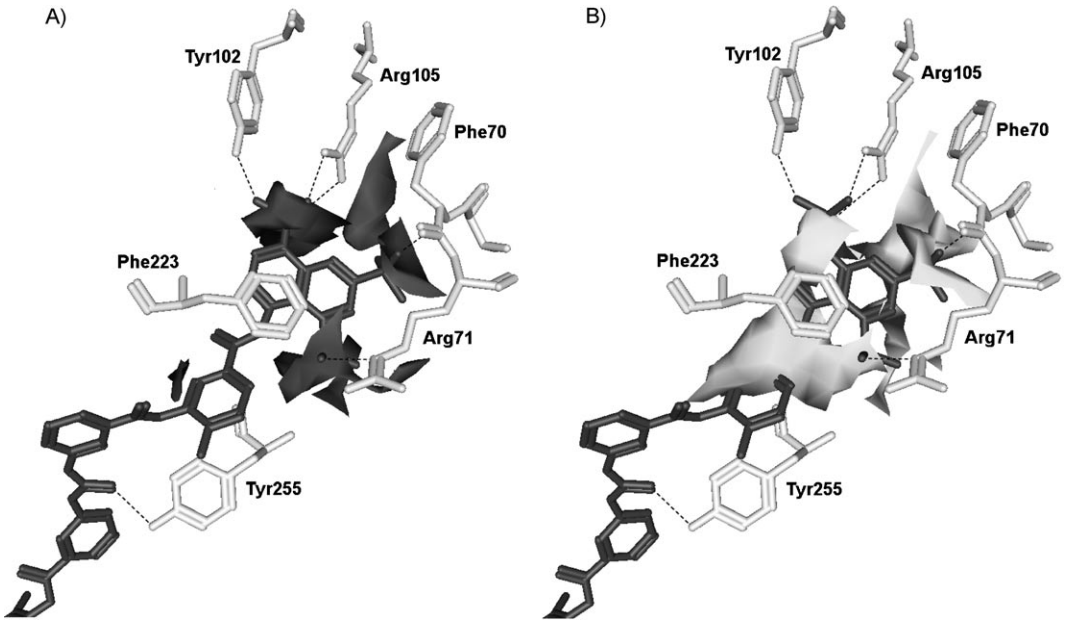

Figure 8. Favorable GRID interaction fields for the SIRT5 binding pocket (PDB code: 2NYR). Field obtained with: A) carboxyl probe (dark gray, contoured at -5.5 kcal mol^{-1}) and B) aromatic probe (light gray, contoured at -2.2 kcal mol^{-1}). Hydrogen bonds between suramin (dark gray sticks) and SIRT5 are displayed as dashed lines (black).

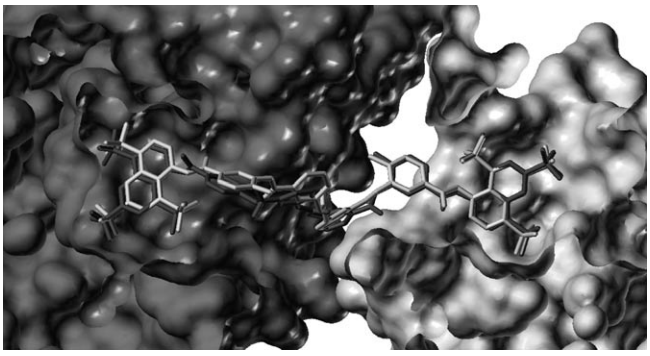

Figure 9. X-ray crystal structure of the SIRT5–suramin complex (PDB code: 2NYR; suramin, white atoms) and the top-ranked docking solution derived for suramin (dark gray atoms). The Connolly surface of the two binding pockets are colored gray (chain A) and white (chain B).

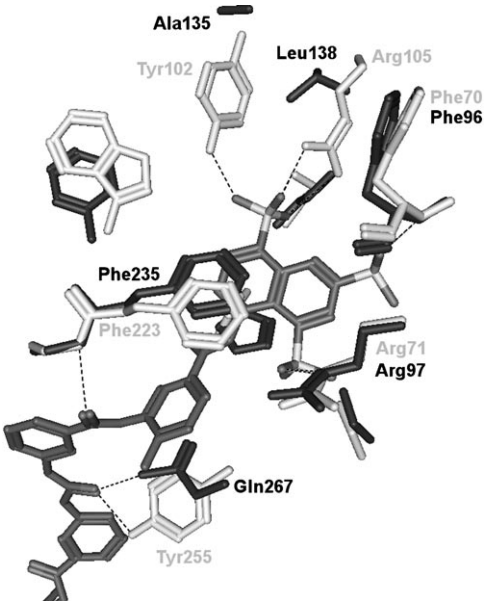

Figure 10. Interaction of suramin (gray) with amino acid residues of the SIRT5 binding pocket (white atoms). For comparison, the corresponding amino acid residues of the SIRT2 model are shown in dark gray atoms. Hydrogen bonds between suramin and the enzyme are displayed as dashed lines (black).

groups of the inhibitors. Whereas a specific interaction could be obtained for one half of the suramin structure, no significant interaction pattern for the second half of the molecule could be observed. From the active compound **14a**, which represents one half of suramin, it is known that this part of the molecule still leads to SIRT2 inhibition in the low micromolar range. (Figure 12A). The docking results show that the suramin derivatives interact in a similar way with SIRT2. However, based on the docking results (GoldScore), no correlation could be derived between scores and IC_{50} values. This is often observed when dealing with docking scores.[30] Therefore, we focused on a qualitative analysis of key interactions necessary for high inhibitory activity.

Docking solutions for the most active compounds **5a**–**5i** show that the naphthylsulfonic acid fragment adopts the same position and conformation as observed for suramin (Figure 12B). The additional alkyl, aryl, or halogen substituents of compounds **5a**–**5i** (R in Figure 2) fit into the binding pocket. Bulkier groups would result in a steric clash with the backbone atoms. A 2D representation for the interactions of **14a** is shown in Figure 12C.

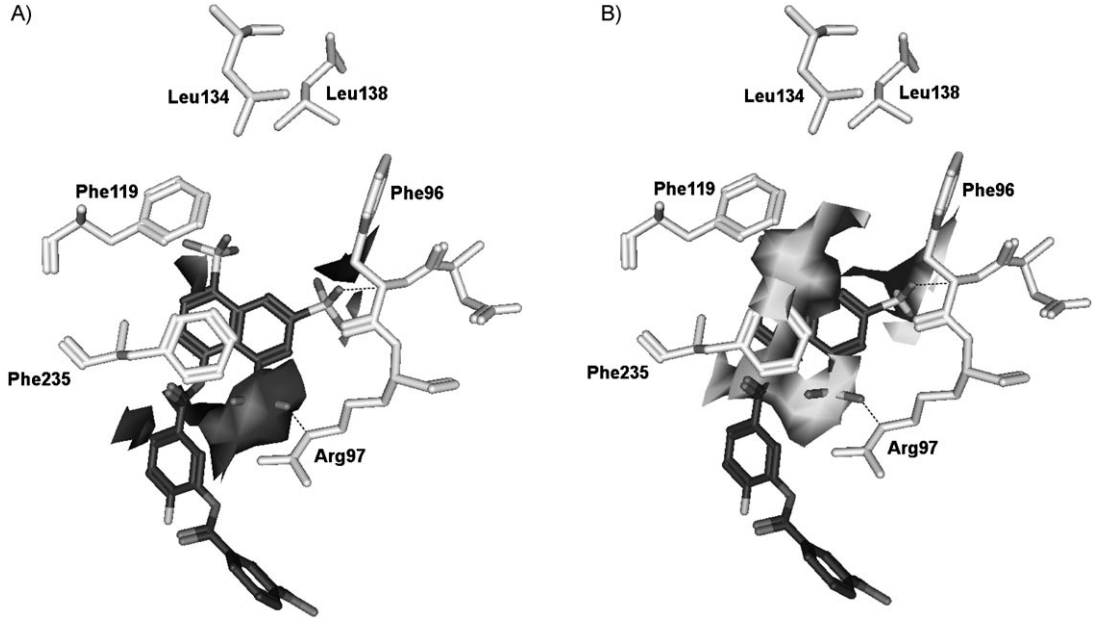

Figure 11. Favorable GRID interaction fields for the SIRT2 model obtained with: A) carboxyl probe (colored dark gray at -3.5 kcal mol^{-1}) and B) aromatic probe (colored light gray at -2.2 kcal mol^{-1}). In addition, the top-ranked docking solution of compound **14a** (dark gray atoms) is displayed. Hydrogen bonds between the inhibitor and SIRT2 are displayed as dashed lines (black).

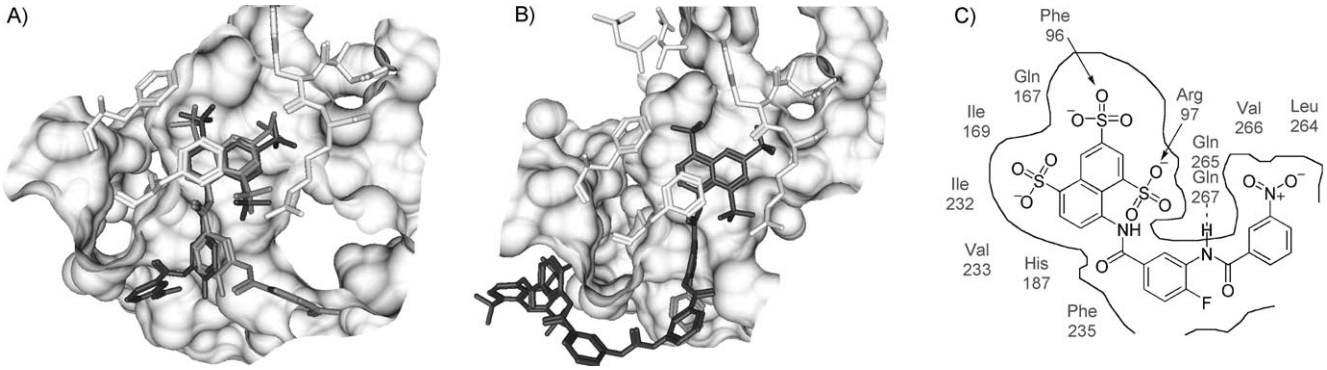

Figure 12. Docking results for suramin derivatives in the SIRT2 model. A) The two top-ranked docking solutions for compound **14a** (dark and light gray atoms). B) Top-ranked docking solution for compound **5b** (dark gray atoms). The additional phenyl substituent of compound **5f** (light gray) as well as the other substituents of the suramin analogues **5a**–**5i** (not shown) fit into the binding pocket. The Connolly surface (calculated with MOE) of the binding pocket is displayed. C) representation of the interaction between **14a** and the SIRT2 model. Hydrogen bonds between inhibitor and enzyme are marked by arrows.

Competition analysis

Besides molecular modeling, the binding mode of suramin **5a** was also analyzed using competition analysis after a method adopted from Lai et al.[31] The inhibition of SIRT2 by **5a** was tested with increasing concentrations of NAD^+ (250–5000 μM). The amount of enzyme, inhibitor (1.5 μM), and acetylated peptide substrate ZMAL were kept constant. No changes in the inhibitory potency of suramin were observed (Figure 13). Owing to solubility problems, we would be able to perform the same experiment with ZMAL only within a very narrow concentration range, so meaningful results cannot be obtained.

These findings are in agreement with the results from the crystal structures of SIRT5, (which has been cocrystallized with suramin and adenosine-5-diphosphoribose (APR)[32] (Figure 14A) as well with the docking results of NAD^+ and the suramin analogue **14a** at SIRT2 (Figure 14B). The binding of NAD^+ and suramin (as well as all other inhibitors of the suramin type presented herein) take place in two different subpockets resulting in the noncompetitive binding observed in the competition analysis.

Conclusions

Suramin and related compounds are pleiotropic drugs that are known to target purine binding sites, particularly purinergic receptors (P2X, P2Y). There was initial evidence that they also inhibit NAD^+-dependent histone deacetylases (sirtuins). We performed a systematic study to obtain structure–activity relation-

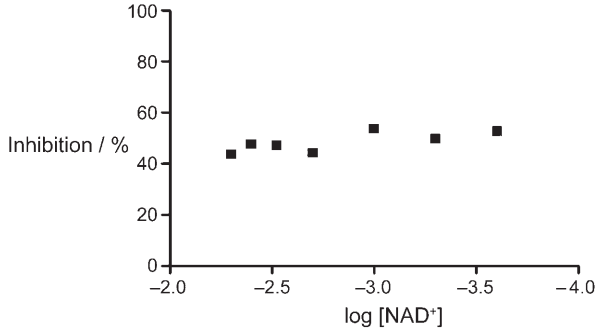

Figure 13. Competition analysis with SIRT2 and suramin (**5a**). The concentration of NAD^+ was varied; all other components were kept constant.

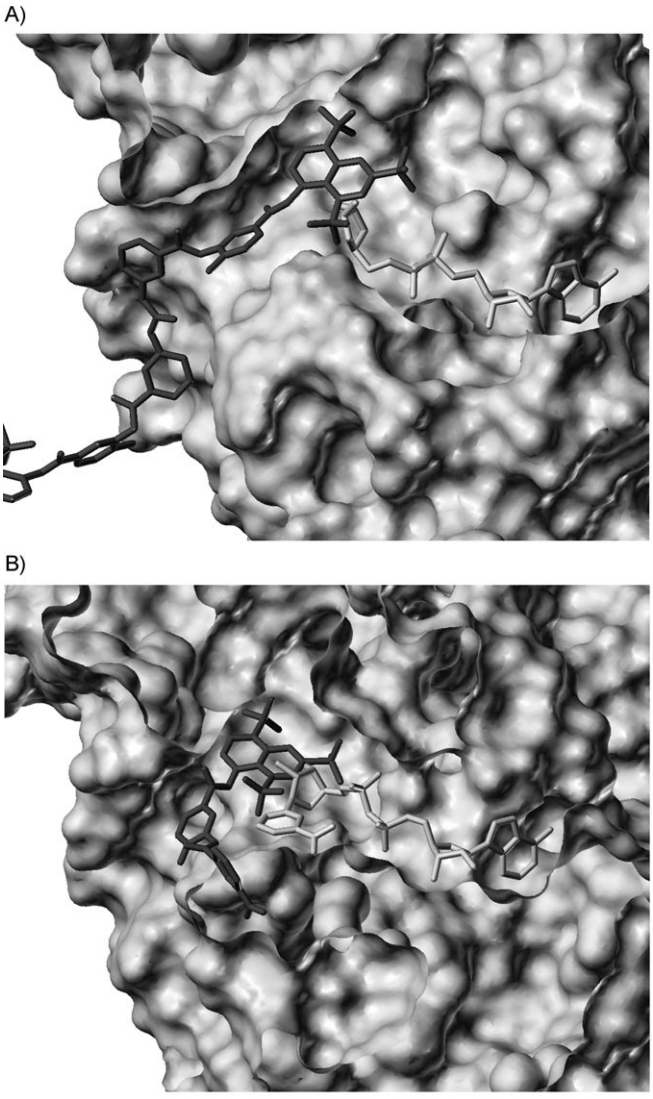

Figure 14. Comparison of suramin and NAD^+ binding site at sirtuins. A) Superimposition of SIRT5 X-ray crystal structures[32] in complex with suramin (dark gray atoms, PDB code: 2NYR) and adenosine-5-diphosphoribose (white atoms, PDB code: 2B4Y). B) GOLD docking results for suramin derivative **14a** (dark gray atoms) and NAD^+ (white atoms) at human SIRT2 (PDB code: 1J8F). The displayed docking solution for NAD^+ resembles the nonproductive NAD^+ conformation observed in the archaeal Sir2-Af2 crystal structure (PDB code: 1YC2).[27]

ships and report detailed inhibition data for human SIRT1 and 2. We found new and potent sirtuin inhibitors that have a preference mainly for SIRT1. The aminoanthranilic acid derivative NF675 (**6c**) is, with an IC_{50} value of 93 nM, together with some similarly potent indoles such as **3**, the most potent sirtuin inhibitor described so far. Notably, its nitro congener **6b** inhibits both SIRT1 and SIRT2 to a much lesser extent. The most selective compound is the "small urea" **7d** (>170-fold selectivity), which is still a very potent SIRT1 inhibitor (466 nM). Sirtuins are so far described to be intracellular, even nuclear enzymes, and the cellular uptake of these highly polar sulfonic acids is generally quite limited. Therefore, the new inhibitor will most likely not be used for studies aimed at therapeutic use. However, the developed inhibitors represent valuable tools with pronounced selectivity for the exploration of the significance of polar motifs in new sirtuin inhibitors that exploit the same binding pocket. For the first time, data are presented that support the presence of a suramin binding site in SIRT2 that is similar to the one experimentally determined for SIRT5, and that compounds which bind to this site can be potent and selective inhibitors of SIRT2. A similar binding site and a similar potential for new drugs may be postulated as well for SIRT1. More drug-like inhibitors that address those sites could be interesting potential drugs for the treatment of HIV or cancer, and our study opens up an avenue to a rational approach in that direction. Our established SARs on SIRT1 and competition analysis results will also be helpful for the generation and validation of SIRT1 protein models.

In addition, taking together the data from the competition experiments on the bis(indolyl)maleimides and the suramin derivatives, as well as the docking results at SIRT2 for both classes of compounds, we were able to show a difference in the interaction mode of sirtuin inhibitors from different structural classes. Such data are very limited so far. This will be helpful for the further establishment of structure–activity relationships and the structure-guided optimization of sirtuin inhibitors.

Experimental Section

Inhibitors: All of the compounds tested were synthesized according to methods previously published by Kassack et al.[18] and Ullmann et al.[19] Analytical data of **5a**–**5i**, **7a**–**7e**, and **14a**,**b** are given in Ullmann et al.[19] Analytical data of compounds **6a**–**c**, **8a**–**13b**, and **15** are presented below. Sirtinol (**1**) was purchased from Axxora, Ro31-8220 (**4**) from Biomol, and AMI-1 (**16**) from Chembridge. If elemental analyses fell outside the 0.4% margin, we determined purity by HPLC and DAD detection using a published protocol.[33] All inhibitors were >90% pure, most of them >95%.

4,4′-(Isophthaloylbis(imino-3,1-(4-methylphenylene)carbonylimino))bis(naphthalene-2,6-disulfonic acid) tetrasodium salt (NF342, 6a): Yield: 54.9%; ^{1}H NMR ([D$_6$]DMSO): δ=10.51 (s, 2H, NH, ex), 10.35 (s, 2H, NH, ex), 8.68 (s, 1H, ar), 8.24–8.21 (m, 4H, ar), 8.09–8.06 (m, 4H, ar), 7.96 (d, 4H, ar, J=8.8 Hz), 7.76–7.72 (m, 5H, ar), 7.49 (d, 2H, ar, J=8.2 Hz), 2.38 ppm (s, 6H, -CH$_3$); ^{13}C NMR ([D$_6$]DMSO): δ=165.8 (2C, ar, C=O), 165.2 (2C, ar, C=O), 146.0 (2C, ar, C-S), 145.7 (2C, ar, C-N), 138.4 (2C, ar, C-S), 136.7 (2C, ar, C-C), 134.8 (2C, ar, C-N), 134.6 (2C, ar, C-C), 132.9 (2C, ar, C-C), 132.5 (2C,

ar, C-C), 131.0 (1C, ar, C-H), 130.9 (2C, ar, C-H), 130.6 (2C, ar, C-H), 128.9 (2C, ar, C-H), 128.6 (2C, ar, C-H), 127.4 (1C, ar, C-H), 126.5 (2C, ar, C-H), 125.6 (2C, ar, C-C), 124.6 (2C, ar, C-H), 122.8 (2C, ar, C-H), 122.6 (2C, ar, C-H), 119.9 (2C, ar, C-H), 18.3 ppm (2C, -CH_3); NaCl: 8.4%; ESMS (positive mode): calcd/found (*m/z*): 1091.0/1091.8 [$M+H]^+$, 1048.0/1047.5 [$M-2Na+3H]^+$, 1025.0/1025.5 [$M-3Na+4H]^+$; ESMS (negative mode): calcd/found (*m/z*): 1067.0/1067.8 [$M-Na]^-$, 1023.0/1023.8 [$M-3Na+2H]^-$, 1001.0/1001.7 [$M-4Na+3H]^-$; anal. ($C_{44}H_{30}N_4O_{16}S_4Na_4$) calcd/found C: 42.3/42.3, H: 2.9/3.2, N: 4.5/4.5.

8,8′-(5-Nitroisophthaloylbis(imino-3,1-phenylencarbonylimino))-bis(naphthalene-1,3,5-trisulfonic acid) hexasodium salt (NF674, 6b): Yield: 97.9%; ^{1}H NMR ([D$_6$]DMSO): $\delta=12.66$ (s, 2H, NH, ex), 10.92 (s, 2H, NH, ex), 9.35 (d, 2H, $J=1.9$ Hz), 9.09 (d, 1H, ar, $J=1.3$ Hz), 9.03 (d, 2H, ar, $J=1.3$ Hz), 8.60 (d, 2H, ar, $J=1.9$ Hz), 8.34 (d, 2H, ar, $J=1.9$ Hz), 7.93–8.11 (m, 8H, ar), 7.51 ppm (t, 2H, ar, $J=7.9$ Hz); ^{13}C NMR ([D$_6$]DMSO): $\delta=165.02$ (2C, C=O), 162.7 (2C, C=O), 147.7 (1C, ar, C-N), 142.4 (2C, ar, C-S), 141.6 (2C, ar, C-N), 141.2 (2C, ar, C-S), 138.3 (2C, ar, C-C), 136.3 (2C, ar, C-S), 136.2 (2C, ar, C-C), 134.3 (2C, ar, C-N), 132.9 (1C, ar, C-H), 131.1 (2C, ar, C-C), 128.2 (2C, ar, C-H), 126.5 (2C, ar, C-H), 125.5 (2C, ar, C-H), 125.0 (2C, ar, C-H), 124.8 (2C, ar, C-H), 123.6 (2C, ar, C-H), 123.1 (2C, ar, C-C), 123.0 (2C, ar, C-H), 122.6 (2C, ar, C-H), 120.6 ppm (2C, ar, C-H); IR ν_{max} (KBr): 4320, 3080, 1650, 1580, 1520, 1480, 1425, 1330, 1180, 1070, 1035, 900, 840, 800, 740, 720, 690, 660 cm^{-1}; NaCl: 14.9%; ESMS (positive mode): calcd/found (*m/z*): 1311.8/1312.2 [$M+H]^+$, 1289.9/1290.1 [$M-Na+2H]^+$, 1267.9/1268.2 [$M-2Na+3H]^+$, 1245.9/1246.1 [$M-3Na+4H]^+$; ESMS (negative mode): calcd/found (*m/z*): 1309.8/1310.1 [$M-H]^-$.

8,8′-(5-Aminoisophthaloylbis(imino-3,1-phenylencarbonylimino))bis(naphthalene-1,3,5-trisulfonic acid) hexasodium salt (NF675, 6c): Yield: 82.3%; ^{1}H NMR ([D$_6$]DMSO): $\delta=12.37$ (s, 2H, NH, ex), 10.39 (s, 2H, NH, ex), 9.42 (d, 2H, ar, $J=2.1$ Hz), 8.64 (d, 2H, ar, $J=2.1$ Hz), 8.39 (d, 2H, ar, $J=1.0$ Hz), 7.79–8.10 (m, 8H, ar), 7.74 (d, 1H, ar, $J=1.0$ Hz), 7.47 (t, 2H, ar, $J=8.1$ Hz), 7.34 (d, 2H, ar, $J=1.0$ Hz), 5.57 ppm (s, 2H, -NH_2, ex); ^{13}C NMR ([D$_6$]DMSO): $\delta=$ 165.7 (2C, C=O), 165.4 (2C, C=O), 148.7 (1C, ar, C-N), 142.3 (2C, ar, C-S), 141.5 (2C, ar, C-N), 141.2 (2C, ar, C-S), 138.9 (2C, ar, C-C), 136.1 (2C, ar, C-S), 135.8 (2C, ar, C-C), 134.4 (2C, ar, C-N), 131.1 (2C, ar, C-C), 127.9 (2C, ar, C-H), 126.5 (2C, ar, C-H), 125.4 (2C, ar, C-H), 124.8 (2C, ar, C-H), 123.1 (2C, ar, C-C), 122.9 (2C, ar, C-H), 122.8 (2C, ar, C-H), 122.6 (2C, ar, C-H), 120.4 (2C, ar, C-H), 115.7 (2C, ar, C-H), 113.9 ppm (1C, ar, C-H); IR ν_{max} (KBr): 3450, 3100, 1660, 1590, 1550, 1480, 1430, 1330, 1300, 1190, 1075, 1040, 890, 840, 800, 730, 690, 660 cm^{-1}; NaCl: 3.2%; anal. ($C_{42}H_{25}N_5Na_6O_{22}S_6$) calcd/found C: 34.7/34.7, H: 2.7/3.1, N: 4.8/4.9.

8,8′-(Carbonylbis(imino-3,1-phenylenecarbonylimino-3,1-(4-methylphenylene)carbonylimino))bis(3-methoxynaphthalene-1,6-disulfonic acid) tetrasodium salt (NF763, 8a): Yield: 83.9%; ^{1}H NMR ([D$_6$]DMSO): $\delta=12.35$ (s, 2H, NH, ex), 10.05 (s, 2H, NH, ex), 9.70 (s, 2H, NH, ex), 8.28 (d, 2H, ar, $J=1.9$ Hz), 8.05 (dd, 2H, ar, $J=4.7$, 1.5 Hz), 8.02 (d, 2H, ar, $J=1.4$ Hz), 7.98 (d, 2H, ar, $J=1.3$ Hz), 7.94 (d, 2H, ar, $J=2.8$ Hz), 7.93 (d, 2H, ar, $J=1.8$ Hz), 7.79 (dd, ar, 2H, $J=6.9$, 1.8 Hz), 7.63 (d, 2H, ar, $J=7.8$ Hz), 7.46 (d, 2H, ar, $J=2.8$ Hz), 7.42 (d, 2H, ar, $J=8.0$ Hz), 7.38 (d, 2H, ar, $J=8.2$ Hz), 3.88 (s, 6H, -OCH_3), 2.31 ppm (s, 6H, -CH_3); ^{13}C NMR ([D$_6$]DMSO): $\delta=$ 165.2 (2C, C=O), 164.5 (2C, ar, C=O), 154.7 (2C, ar, C-O), 152.5 (1C, C=O), 144.8 (2C, ar, C-S), 143.4 (2C, ar, C-N), 139.8 (2C, ar, C-N), 136.9 (2C, ar, C-N), 136.6 (2C, ar, C-S), 136.1 (2C, ar, C-C), 135.1 (2C, ar, C-C), 133.6 (2C, ar, C-C), 133.1 (2C, ar, C-C), 129.6 (2C, ar, C-H), 128.5 (2C, ar, C-H), 126.4 (2C, ar, C-H), 123.7 (2C, ar, C-H), 121.0 (2C, ar, C-H), 120.8 (2C, ar, C-H), 120.6 (2C, ar, C-H), 120.0 (2C, ar, C-H), 119.1 (2C, ar, C-H), 117.9 (2C, ar, C-C), 117.4 (2C, ar, C-H), 109.9 (2C, ar, C-H), 55.3 (2C, -OCH_3), 17.9 ppm (2C, -CH_3); IR ν_{max} (KBr): 3448, 2922, 1654, 1647, 1618, 1592, 1542, 1534, 1484, 1375, 1305, 1233, 1193, 1039, 981, 887, 803, 749, 691, 623, 512 cm^{-1}; NaCl: 5.9%; ESMS (positive mode): calcd/found (*m/z*): 1285.0/1285.3 [$M+H]^+$, 1263.1/1263.0 [$M-Na+2H]^+$.

7,7′-(Carbonylbis(imino-3,1-phenylenecarbonylimino-3,1-(4-methylphenylene)carbonylimino))bis(1-methoxynaphthalene-3,6-disulfonic acid) tetrasodium salt (NF770, 8b): Yield: 28.0%; ^{1}H NMR ([D$_6$]DMSO): $\delta=11.41$ (s, 2H, NH, ex), 10.12 (s, 2H, NH, ex), 10.12 (s, 2H, NH, ex), 9.27 (d, 2H, ar, $J=2.1$ Hz), 8.26 (s, 2H, ar), 8.12 (d, 2H, ar, $J=1.2$ Hz), 8.00 (d, 2H, ar, $J=1.4$ Hz), 7.81 (d, 2H, ar, $J=7.7$ Hz), 7.75 (d, 2H, ar, $J=7.4$ Hz), 7.65 (d, 2H, ar, $J=2.1$ Hz), 7.62 (d, 2H, ar, $J=8.0$ Hz), 7,50 (t, 2H, ar, $J=8.3$ Hz), 7.43 (d, 2H, ar, $J=7.9$ Hz), 7.20 (d, 2H, ar, $J=1.2$ Hz), 4.02 (s, 6H, -OCH_3), 2.35 ppm (s, 6H, -CH_3); ^{13}C NMR ([D$_6$]DMSO): $\delta=165.5$ (2C, C=O), 163.4 (2C, C=O), 153.7 (2C, C-O),152.7 (1C, C=O), 144.7 (2C, ar, C-S), 140.1 (2C, ar, C-N), 138.0 (2C, ar, C-S), 136.9 (2C, ar, C-N), 134.9 (2C, ar, C-C), 136.3 (2C, ar, C-N), 132.7 (2C, ar, C-C), 132.6 (2C, ar, C-C), 130.5 (2C, ar, C-H), 128.5 (2C, ar, C-H), 128.3 (2C, ar, C-C), 126.3 (2C, ar, C-H), 125.5 (2C, ar, C-H), 125.3 (2C, ar, C-C), 123.7 (2C, ar, C-H), 121.1 (2C, ar, C-H), 120.5 (2C, ar, C-H), 117.5 (2C, ar, C-H), 116.6 (2C, ar, C-H), 110.7 (2C, ar, C-H), 103.2 (2C, ar, C-H), 55.6 (2C, -OCH_3), 18.0 ppm (2C, -CH_3); IR ν_{max} (KBr): 3447, 2925, 1654, 1560, 1458, 1326, 1173, 1100, 1041, 905, 843, 747, 684, 656 cm^{-1}; NaCl: 8.3%; ESMS (positive mode): calcd/found (*m/z*): 1285.1/1285.5 [$M+H]^+$, 1263.1/1263.5 [$M-Na+2H]^+$.

4,4′-(Carbonylbis(imino-3,1-(4-methylphenylene)carbonylimino))-bis(naphthalene-1,5-disulfonic acid) tetrasodium salt (NF290, 9a). Yield: 82.9%; ^{1}H NMR ([D$_6$]DMSO): $\delta=12.52$ (s, 2H, NH, ex), 9.09 (dd, 2H, ar, $J=8.5$, 1.3 Hz), 8.64 (s, 2H, NH, ex), 8.34 (d, 2H, ar, $J=1.3$ Hz), 8.28 (dd, 2H, ar, $J=7.2$, 1.3 Hz), 8.02 (s, 4H, ar), 7.86 (dd, 2H, ar, $J=7.9$, 1.6 Hz), 7.44 (dd, 2H, ar, $J=8.5$, 7.6 Hz), 7.28 (d, 2H, ar, $J=8.2$ Hz), 2.38 ppm (s, 6H, -CH_3); ^{13}C NMR ([D$_6$]DMSO): $\delta=$ 165.7 (2C, C=O), 153.3 (1C, C=O), 141.9 (2C, ar, C-H), 141.1 (2C, ar, C-C), 137.5 (2C, ar, C-N), 134.8 (2C, ar, C-S), 133.9 (2C, ar, C-S), 132.3 (2C, ar, C-C), 131.7 (2C, ar, C-C), 130.8 (2C, ar, C-H), 129.8 (2C, ar, C-H), 127.1 (2C, ar, C-H), 124.7 (2C, ar, C-H), 123.6 (2C, ar, C-H), 123.5 (2C, ar, C-H), 122.7 (2C, ar, C-C), 122.5 (2C, ar, C-H), 122.4 (2C, ar, C-H), 18.4 ppm (2C, -CH_3); NaCl: 15.4%; ESMS (positive mode): calcd/found (*m/z*): 1009.0/1009.0 [$M+Na]^+$, 987.0/987.0 [$M+H]^+$, 965.0/965.0 [$M-Na+2H]^+$; anal. ($C_{37}H_{26}N_4Na_4O_{15}S_4$): calcd/found C:31.7/31.7, H: 3.4/3.6, N: 4.0/3.9.

5,5′-(Carbonylbis(imino-3,1-(4-methylphenylene)carbonylimino))-bis(2-methoxynaphthalene-4,7-disulfonic acid) tetrasodium salt (NF762, 9b): Yield: 91.0%; ^{1}H NMR ([D$_6$]DMSO): $\delta=12.28$ (s, 2H, NH, ex), 8.57 (s, 2H, NH, ex), 8.33 (d, 2H, ar, $J=1.6$ Hz), 8.27 (d, 2H, ar, $J=1.9$ Hz), 7.94 (d, 2H, ar, $J=1.6$ Hz), 7.93 (s, 2H, ar), 7.86 (dd, 2H, ar, $J=8.0$, 1.6 Hz), 7.46 (d, 2H, ar, $J=2.9$ Hz), 7.29 (d, 2H, ar, $J=8.3$ Hz), 3.89 (s, 6H, -OCH_3), 2.37 ppm (s, 6H, -CH_3); ^{13}C NMR ([D$_6$]DMSO): $\delta=165.0$ (2C, C=O), 154.7 (2C, C-O), 152.9 (1C, C=O), 144.6 (2C, ar, C-S), 143.4 (2C, ar, C-N), 137.0 (2C, ar, C-N), 136.6 (2C, ar, C-S), 133.8 (2C, ar, C-C), 133.3 (2C, ar, C-C), 132.2 (2C, ar, C-C), 129.4 (2C, ar, C-H), 122.5 (2C, ar, C-H), 122.3 (2C, ar, C-H), 120.9 (2C, ar, C-H), 120.0 (2C, ar, C-H), 119.0 (2C, ar, C-H), 118.0 (2C, ar, C-C), 109.9 (2C, ar, C-H), 55.3 (2C, -OCH_3), 18.1 ppm (2C, -CH_3); IR ν_{max} (KBr): 3448, 1624, 1577, 1543, 1450, 1374, 1235, 1187, 1044, 985, 769, 753, 631 cm^{-1}; NaCl: 5.5%; ESMS (positive mode): calcd/found (*m/z*): 1069.0/1069.4 [$M+Na]^+$, 1047.0/1047.5 [$M+H]^+$; anal. ($C_{39}H_{30}N_4Na_4O_{17}S_4$) calcd/found C: 34.8/34.9, H: 4.1/4.4, N: 4.2/4.1.

7,7′-(Carbonylbis(imino-3,1-(4-methylphenylene)carbonylimino))-bis(1-methoxynaphthalene-3,6-disulfonic acid) tetrasodium salt

(NF769, 9c): Yield: 65.1%; ^{1}H NMR ([D$_6$]DMSO): δ = 11.30 (s, 2H, NH, ex), 9.27 (d, 2H, ar, J = 2.1 Hz), 9.06 (s, 2H, NH, ex), 8.48 (d, 2H, ar, J = 1.5 Hz), 8.24 (s, 2H, ar), 7.72 (d, 2H, ar, J = 1.2 Hz), 7.59 (dd, 2H, ar, J = 8.0, 1.7 Hz), 7.38 (d, 2H, ar, J = 8.1 Hz), 7.18 (d, 2H, ar, J = 1.2 Hz), 4.01 (s, 6H, -OCH$_3$), 2.43 ppm (s, 6H, -CH$_3$); ^{13}C NMR ([D$_6$]DMSO): δ = 163.9 (2C, C=O), 153.7 (2C, ar, C-O), 152.9 (1C, C=O), 144.6 (2C, ar, C-S), 137.9 (2C, ar, C-S), 136.3 (2C, C-N), 132.8 (2C, ar, C-N), 132.7 (2C, ar, C-C), 132.7 (2C, ar, C-C), 130.2 (2C, ar, C-H), 128.2 (2C, ar, C-C), 126.3 (2C, ar, C-H), 125.3 (2C, ar, C-C), 121.2 (2C, ar, C-H), 120.4 (2C, ar, C-H), 116.6 (2C, ar, C-H), 110.7 (2C, ar, C-H), 103.2 (2C, ar, C-H), 55.6 (2C, -OCH$_3$), 18.4 ppm (2C, -CH$_3$); IR ν_{max} (KBr): 3459, 2951, 2852, 1664, 1542, 1457, 1413, 1365, 1328, 1181, 1126, 1103, 1048, 1011, 971, 909, 838, 8140, 748, 686, 659, 619, 585, 541 cm^{-1}; UV ε_{max} = 228, 264, 318 nm; NaCl: 18.3%; ESMS (positive mode): calcd/found (*m/z*): 1069.0/1069.4 [M+Na]$^+$, 1047.0/1047.4 [M+H]$^+$; ESMS (negative mode): calcd/found (*m/z*): 1045.0/1045.4 [M−H]$^-$, 1023.0/1023.5 [M−Na]$^-$, 1001.4/1001.0 [M−2Na+H]$^-$; anal. ($C_{39}H_{30}N_4Na_4O_{17}S_4$) calcd/found C: 27.0/27.0, H: 4.1/4.1, N: 3.2/3.2.

8,8′-(Carbonylbis(imino-4,2′-biphenylenecarbonylimino))bis-(naphthalene-1,3,5-trisulfonic acid) hexasodium salt (NF136, 10): Yield: 68.5%; ^{1}H NMR ([D$_6$]DMSO): δ = 12.66 (s, 2H, NH, ex), 9.37 (s, 2H, ar), 8.72 (s, 2H, NH, ex), 8.61 (s, 2H, ar), 8.04 (d, 2H, ar, J = 8.2 Hz), 8.01 (d, 2H, ar, J = 8.5 Hz), 7.91 (d, 2H, ar, J = 7.3 Hz), 7.37–7.50 ppm (m, 14H, ar); ^{13}C NMR ([D$_6$]DMSO): δ = 167.9 (2C, C=O), 152.6 (1C, C=O), 142.8 (2C, ar, C-N), 141.7 (2C, ar, C-S), 141.5 (2C, ar, C-N), 139.9 (2C, ar, C-S), 138.9 (2C, ar, C-C), 137.4 (2C, ar, C-H), 135.0 (2C, ar, C-S), 134.5 (2C, ar, C-C), 131.4 (2C, ar, C-C), 129.8 (2C, ar, C-C), 129.5 (2C, ar, C-H), 129.1 (4C, ar, C-H), 128.6 (2C, ar, C-H), 126.7 (2C, ar, C-H), 126.5 (2C, ar, C-H), 125.7 (2C, ar, C-H), 125.2 (2C, ar, C-H), 122.7 (2C, ar, C-C), 120.6 (2C, ar, C-H), 118.1 ppm (4C, ar, C-H); ESMS (positive mode): calcd/found (*m/z*): 1314.9/1315.2 [M+H]$^+$, 1292.9/1293.2 [M−Na+2H]$^+$, ESMS (negative mode): calcd/found (*m/z*): 1290.9/1291.6 [M−Na]$^-$, 1249.0/1249.1 [M−3Na+4H]$^+$.

3,3′,3″,3‴-(Terephthaloylbis(imino-2,1,4-benzenetriylbis(carbonyliminomethylene)))tetrakisbenzenesulfonic acid tetrasodium salt (NF444, 11): Yield: 40.0%; ^{1}H NMR ([D$_6$]DMSO): δ = 12.52 (s, 2H, NH, ex), 9.57 (t, 2H, NH, ex, J = 6.0 Hz), 9.25 (t, 2H, NH, ex, J = 6.0 Hz), 9.08 (d, 2H, ar, J = 1.6 Hz), 8.10 (s, 4H, ar), 7.99 (d, 2H, ar, J = 8.5 Hz), 7.71 (dd, 2H, ar, J = 8.5, 1.6 Hz), 7.66 (s, 2H, ar), 7.62 (s, 2H, ar), 7.51–7.48 (m, 4H, ar), 7.33–7.27 (m, 8H, ar), 4.54 (d, 4H, -CH$_2$-, J = 5.7 Hz), 4.50 ppm (d, 4H, -CH$_2$-, J = 5.7 Hz); ^{13}C NMR ([D$_6$]DMSO): δ = 167.7 (2C, C=O), 165.2 (2C, C=O), 163.6 (2C, C=O), 147.8 (4C, ar, C-S), 138.9 (2C, ar, C-N), 138.8 (2C, ar, C-C), 138.2 (2C, ar, C-C), 137.5 (2C, ar, C-C), 137.3 (2C, ar, C-C), 127.5 (4C, ar, C-H), 127.5 (4C, ar, C-H), 127.4 (4C, ar, C-H), 124.4 (4C, ar, C-H), 124.1 (2C, ar, C-H), 123.9 (2C, ar, C-H), 122.7 (2C, ar, C-C), 121.5 (2C, ar, C-H), 120.0 (2C, ar, C-H), 120.0 (2C, ar, C-H), 42.7 ppm (4C, -CH$_2$-); IR ν_{max} (KBr): 3420, 1640, 1600, 1570, 1540, 1450, 1430, 1320, 1280, 1200, 1110, 1040, 990, 720, 680 cm^{-1}; ESMS (positive mode): calcd/found (*m/z*): 1279.1/1279.4 [M+Na]$^+$, 1191.2/1191.3 [M−3Na+4H]$^+$; ESMS (negative mode): calcd/found (*m/z*): 1233.1/1233.7 [M−Na]$^-$, 1255.1/1255.7 [M−H]$^-$.

8,8′-(Terephthaloylbis(imino-4,1-phenylenecarbonylimino))bis-(naphthalene-1,3,5-trisulfonic acid) hexasodium salt (NF343, 12): Yield: 43.2%; ^{1}H NMR ([D$_6$]DMSO): δ = 12.59 (s, 2H, NH, ex), 10.68 (s, 2H, NH, ex), 9.40 (d, 2H, ar, J = 2.2 Hz), 8.63 (d, 2H, ar, J = 1.9 Hz), 8.17 (s, 4H, ar), 8.17 (d, 4H, ar, J = 8.5 Hz), 8.08 (d, 2H, ar, J = 8.5 Hz), 8.06 (d, 2H, ar, J = 8.5 Hz), 7.95 ppm (d, 4H, ar, J = 8.8 Hz); ^{13}C NMR ([D$_6$]DMSO): δ = 165.3 (2C, C=O), 165.1 (2C, C=O), 142.8 (2C, ar, C-N), 141.9 (2C, ar, C-S), 141.7 (2C, ar, C-N), 141.5 (2C, ar, C-C), 137.6 (2C, ar, C-S), 134.6 (2C, ar, C-S), 131.5 (2C, ar, C-C), 130.9 (2C, ar, C-C), 129.0 (4C, ar, C-H), 128.1 (4C, ar, C-H), 126.9 (2C, ar, C-H), 125.9 (2C, ar, C-H), 125.0 (2C, ar, C-H), 123.3 (2C, ar, C-C), 122.6 (2C, ar, C-H), 119.5 ppm (4C, ar, C-H); NaCl: 20.0%; ESMS (negative mode): calcd/found (*m/z*): 1264.8/1265.5, [M−H]$^-$, 1243.9/1243.5 [M−Na]$^-$; anal. ($C_{42}H_{24}N_4O_{22}S_6Na_6$) calcd/found: C:30.3/30.3, H: 1.9/1.9, N: 3.4/3.4.

3,3′,3″,3‴-(Isophthaloylbis(imino-2,1,4-benzenetriylbis(carbonyliminomethylene)))tetrakisbenzenesulfonic acid tetrasodium salt (NF443, 13a): Yield: 93.0%; ^{1}H NMR ([D$_6$]DMSO): δ = 12.56 (s, 2H, NH, ex), 9.57 (t, 2H, NH, ex, J = 6.0 Hz), 9.25 (t, 2H, NH, ex, J = 6.0 Hz), 8.98 (d, 2H, ar, J = 1.6 Hz), 8.57 (dd, 1H, ar, J = 1.6 Hz), 8.13 (dd, 2H, ar, J = 7.9, 1.6 Hz), 8.00 (d, 2H, ar, J = 7.9 Hz), 7.89 (d, 1H, ar, J = 7.9 Hz), 7.73 (dd, 2H, ar, J = 1.6, 7.9 Hz), 7.66 (d, 2H, ar, J = 2.2 Hz), 7.64 (d, 2H, ar, J = 2.2 Hz), 7.52–7.53 (m, 4H, ar), 7.28–7.33 (m, 8H, ar), 4.54 (d, 4H, -CH$_2$-, J = 5.7 Hz), 4.51 ppm (d, 4H, -CH$_2$-, J = 5.7 Hz); ^{13}C NMR ([D$_6$]DMSO): δ = 167.9 (2C, C=O), 163.8 (2C, C=O), 165.4 (2C, C=O), 148.1 (2C, ar, C-S), 148.0 (2C, ar, C-S), 139.1 (2C, ar, C-N), 138.9 (2C, ar, C-C), 138.3 (2C, ar, C-C), 137.7 (2C, ar, C-C), 135.1 (2C, ar, C-C), 129.8 (2C, ar, C-H), 129.5 (1C, ar, C-H), 127.6 (4C, ar, C-H), 127.5 (4C, ar, C-H), 126.7 (1C, ar, C-H), 126.2 (2C, ar, C-H), 124.6 (4C, ar, C-H), 124.2 (2C, ar, C-H), 124.1 (2C, ar, C-H), 122.9 (2C, ar, C-C), 121.6 (2C, ar, C-H), 120.1 (2C, ar, C-H), 42.7 ppm (4C, -CH$_2$-); IR ν_{max} (KBr): 3430, 1650, 1610, 1580, 1540, 1450, 1430, 1390, 1360, 1330, 1200, 1110, 1040, 720, 690 cm^{-1}; ESMS (positive mode): calcd/found (*m/z*): 1279.1/1279.3 [M+Na]$^+$; ESMS (negative mode): calcd/found (*m/z*): 1255.1/1255.8 [M−H]$^-$, 1233.1/1233.7 [M−Na]$^-$.

3,3′,3″,3‴-(Isophthaloylbis(imino-5,1,3-benzenetriylbis(carbonyliminomethylene)))tetrakisbenzenesulfonic acid tetrasodium salt (NF451, 13b): Yield: 79.0%; ^{1}H NMR ([D$_6$]DMSO): δ = 11.60 (s, 2H, NH, ex), 10.68 (s, 2H, NH, ex), 10.57 (s, 2H, NH, ex), 8.85 (d, 2H, ar, J = 1.9 Hz), 8.58 (d, 1H, ar, J = 1.7 Hz), 8.15 (dd, 2H, J = 8.5, 2.2 Hz), 8.12 (d, 2H, J = 2.2 Hz), 8.05 (d, 2H, ar, J = 8.5 Hz), 8.00 (d, 2H, ar, J = 2.2 Hz), 7.91 (dd, 2H, ar, J = 8.5, 1.7 Hz), 7.86 (dd, 2H, ar, J = 7.9, 1.6 Hz), 7.80 (d, 1H, ar, J = 8.5 Hz), 7.77 (dd, 2H, ar, J = 7.9, 1.6 Hz), 7.39–7.42 (m, 4H, ar), 7.37 (d, 2H, ar, J = 8.5 Hz), 7.32 ppm (d, 2H, ar, J = 8.5 Hz), ^{13}C NMR ([D$_6$]DMSO): δ = 166.4 (2C, C=O), 164.5 (2C, C=O), 164.3 (2C, C=O), 148.5 (2C, ar, C-S), 148.4 (2C, ar, C-S), 138.3 (2C, ar, C-N), 137.9 (2C, ar, C-N), 137.9 (2C, ar, C-N), 137.7 (2C, ar, C-C), 135.0 (2C, ar, C-C), 130.1 (2C, ar, C-H), 129.5 (1C, ar, C-H), 129.0 (2C, ar, C-H), 127.9 (4C, ar, C-H), 127.0 (1C, ar, C-H), 126.9 (2C, ar, C-C), 122.7 (2C, ar, C-H), 121.8 (2C, ar, C-H), 121.5 (2C, ar, C-H), 121.2 (4C, ar, C-H), 120.6 (2C, ar, C-H), 118.5 (2C, ar, C-H), 118.0 ppm (2C, ar, C-H); IR ν_{max} (KBr): 3440, 1690, 1640, 1600, 1550, 1530, 1470, 1450, 1420, 1380, 1330, 1200, 1100, 1030, 990, 780, 700, 670 cm^{-1}; ESMS (positive mode): calcd/found (*m/z*): 1179.1/1179.3 [M−Na+2H]$^+$; ESMS (negative mode): calcd/found (*m/z*): 1199.0/1199.4 [M−H]$^-$, 1177.0/1177.6 [M−Na]$^-$.

4,4′-(Carbonylbis(imino-4,1-phenylenemethyleneimino))bis(benzenesulfonic acid) (NF669, 16): Yield: 34.5%; ^{1}H NMR ([D$_6$]DMSO): δ = 9.10 (s, 2H, NH, ex), 7.68 (dd, 2H, NH, J = 8.5, 3.5 Hz), 7.50 (d, 4H, ar, J = 7.6 Hz), 7.42 (d, 4H, ar, J = 8.2 Hz), 7.32–7.28 (m, 6H, ar), 6.95 (s, 4H, ar), 4.32 ppm (s, 4H, -CH$_2$-); ^{13}C NMR ([D$_6$]DMSO): δ = 152.7 (2C, ar, C-N), 147.8 (1C, C=O), 139.7 (2C, ar, C-S), 131.1 (2C, ar, C-C), 129.4 (2C, ar, C-N), 127.2 (8C, ar, C-H), 122.5 (4C, ar, C-H), 118.1 (4C, ar, C-H), 49.96 ppm (2C, -CH$_2$-); ESMS (negative mode): calcd/found (*m/z*): 625.1/625.4 [M+2Na-3H]$^-$, 603.1/603.5 [M+Na-2H]$^-$.

Recombinant proteins: Human SIRT1 (N-terminally GST tagged) was prepared as described previously[25] with minor modifications. Briefly, plasmid pTe34 (a gift from A. Salminen, University of Kuopio, Finland) containing the full-length human SIRT1 cDNA was transformed in *E. coli* BL21 (DE3; Invitrogen) for expression. The

culture was grown in LB medium to an optical density of 0.6 (A_{600}) at 37 °C, induced with isopropyl-β-D-thiogalactopyranoside (IPTG; 0.2 mM) for 4 h, and centrifuged. Lysis was performed with sonication (five 10-s bursts at 60% output (Sonifier 250, Branson) after pre-incubation with lysozyme (1 mg mL^{-1}) for 30 min. The soluble overexpressed protein was purified with Glutathione Sepharose 4B beads (Amersham Biosciences).

Human SIRT2 (N-terminally tagged with His_6) was prepared as described previously with minor modifications. Briefly, plasmid pEV1440 containing the full-length human SIRT2 cDNA was transformed in *E. coli* strain BL21 (DE3) pLysS (Invitrogen) for expression. The culture was grown in LB medium to an optical density of 0.6 (A_{600}) at 37 °C, induced with 0.1 mM IPTG for 2 h, and centrifuged. Lysis was performed with a French press. The soluble overexpressed recombinant protein was purified with Ni-NTA resin.

The identity of the GST–SIRT1 and His_6–SIRT2 proteins produced was verified with SDS-PAGE electrophoresis. Deacetylase activity of the produced enzymes was dependent on NAD^+ and could be inhibited with sirtinol (**1**) and nicotinamide.

Sirtuin assay: All compounds were evaluated for their ability to inhibit recombinant sirtuins using a homogeneous fluorescent deacetylase assay. Stock solutions of inhibitors were prepared in sirtuin buffer. The assay was carried out in 96-well plates: 60 μL reaction volume contained the fluorescent histone deacetylase substrate ZMAL (10.5 μM), NAD^+ (500 μM), and SIRT2 (3 μL) or SIRT1 (2.5 μL). Total substrate conversion was driven to about 10% to assure initial state conditions. After 4 h incubation at 37 °C, the deacetylation reaction was stopped, and the metabolite formed (ZML, the deacetylated form of ZMAL) was developed using a tryptic digest for 20 min to form a different fluorophore. Finally, fluorescence was measured in a plate reader (BMG Polarstar) with excitation at $\lambda = 390$ nm and emission at $\lambda = 460$ nm. The amount of remaining substrate in the positive control with inhibitor versus negative control without inhibitor was employed to calculate inhibition. All IC_{50} determinations were carried out at least in duplicate. All compounds were tested for aminomethylcoumarin (AMC) quenching and trypsin inhibition, but no interference was observed. IC_{50} data were analyzed using GraphPad Prism software.

Molecular modeling: All calculations were performed on a Pentium IV 1.8 GHz based Linux cluster. The molecular structures of the inhibitors were generated using the MOE modeling package (Chemical Computing Group).[34] The structures were energy minimized using the MMFF94s force field and the conjugate gradient method until the default derivative convergence criterion of 0.01 kcal mol^{-1} Å^{-1} was met. The sulfonic acid substituents of the suramin derivatives were considered deprotonated. The crystal structures of human SIRT2 (PDB code: 1J8F),[28] SIRT5 (PDB codes: 2B4Y and 2NYR),[32] and archaeal Sir2-Af2 (PDB code: 1YC2)[27] were taken from the Protein Data Bank.[35] SIRT2 is a monomer in solution, and therefore only one chain was chosen from the trimeric SIRT2 structure of 1J8F. Monomer B was selected for SIRT5 and monomer C for Sir2-Af2, as they showed the best stereochemical quality examined with the program PROCHECK.[36] In addition to the noncomplexed form of human SIRT2, the archaeal Sir2-Af2 and the SIRT5 crystal were taken for the current investigation to determine the NAD^+–enzyme and suramin–enzyme interactions, respectively. Because the X-ray structures might contain residual energetic tension from the crystallization process, the minimized sirtuin structures were used for the docking study. After removing the cocrystallized water molecules and adding hydrogen atoms to the protein structure, a descent minimization using the MMFF94s force field and the GB/SA continuum[37] solvent model for water was carried out. During minimization, a tethering constant of 100 kcal mol^{-1} Å^{-1} was applied on the backbone atoms after a stepwise reduction of the tethering to 1 kcal mol^{-1} Å^{-1}.

For the docking of the suramin derivatives we took the SIRT5 crystal structure and a SIRT2 model that was generated on the basis of human SIRT2 and human SIRT5 cocrystallized with suramin. The coordinates for the flexible loop neighboring the suramin binding site (Figure 10) were adopted from the SIRT5 protein structure, whereas most of the coordinates were taken from the SIRT2 structure. The generated SIRT2 model was energy minimized and equilibrated using molecular dynamics simulations within the GROMACS 3.2.1 program.[38] We applied the same simulation setup as described previously by Poso and co-workers.[10] An equilibration period of 250 ps with constraints of 250 kcal mol^{-1} on the backbone atoms was followed by a free MD simulation for 1 ns. Trajectories of free MD simulations were analyzed using NMRCLUST.[39]

Interaction possibilities were analyzed using the GRID program (Molecular Discovery Inc.). GRID is an approach to predict noncovalent interactions between a molecule of known 3D structure (that is, a sirtuin) and a small group as a probe (representing chemical features of a ligand).[40] The calculations were performed using version 22 of the GRID program and the crystal structures mentioned above. The calculations were performed on a cube ($20 \times 20 \times 20$ Å^3, spacing 1 Å), including the NAD^+ and suramin binding site, to search for binding sites complementary to the functional groups of the inhibitors. The carbonyl and the aromatic probes were used for the analysis. The calculated GRID contour maps were then viewed superimposed on the crystal structure of the particular sirtuin using the MOE software package.

Docking of the cocrystallized suramin as well as the suramin derivatives was carried out using GOLD 3.0.[29] The same docking setup that we previously successfully applied for the docking of bis-(indolyl)maleimide SIRT2 inhibitors was used.[21] All torsion angles in each compound were allowed to rotate freely. GoldScore was chosen as the fitness function. For each molecule, 30 docking runs were performed. The resulting solutions were clustered on the basis of the heavy atom rmsd values (1 Å). The top-ranked poses for each ligand were retained and analyzed together with the GRID interaction fields within MOE.

Keywords: docking · hydrolases · sirtuin inhibitors · structure–activity relationships · suramin

[1] S. Schäfer, M. Jung, *Arch. Pharm.* **2005**, *338*, 347 – 357.
[2] M. Biel, V. Wascholowski, A. Giannis, *Angew. Chem.* **2005**, *117*, 3248 – 3280; *Angew. Chem. Int. Ed.* **2005**, *44*, 3186 – 3216.
[3] B. J. North, E. Verdin, *Genome Biol.* **2004**, *5*, 224.
[4] J. Trapp, M. Jung, *Curr. Drug Targets* **2006**, *7*, 1553 – 1560.
[5] K. J. Bitterman, R. M. Anderson, H. Y. Cohen, M. Latorre-Esteves, D. A. Sinclair, *J. Biol. Chem.* **2002**, *277*, 45099 – 45107.
[6] C. M. Grozinger, E. D. Chao, H. E. Blackwell, D. Moazed, S. L. Schreiber, *J. Biol. Chem.* **2001**, *276*, 38837 – 38843.
[7] A. Mai, S. Massa, S. Lavu, R. Pezzi, S. Simeoni, R. Ragno, F. R. Mariotti, F. Chiani, G. Camilloni, D. A. Sinclair, *J. Med. Chem.* **2005**, *48*, 7789 – 7795.
[8] A. Bedalov, T. Gatbonton, W. P. Irvine, D. E. Gottschling, J. A. Simon, *Proc. Natl. Acad. Sci. USA* **2001**, *98*, 15113 – 15118.
[9] J. Posakony, M. Hirao, S. Stevens, J. A. Simon, A. Bedalov, *J. Med. Chem.* **2004**, *47*, 2635 – 2644.
[10] A. J. Tervo, S. Kyrylenko, P. Niskanen, A. Salminen, J. Leppanen, T. H. Nyronen, T. Jarvinen, A. Poso, *J. Med. Chem.* **2004**, *47*, 6292 – 6298.
[11] A. J. Tervo, T. Suuronen, S. Kyrylenko, E. Kuusisto, P. H. Kiviranta, A. Salminen, J. Leppanen, A. Poso, *J. Med. Chem.* **2006**, *49*, 7239 – 7241.

[12] S. Pagans, A. Pedal, B. J. North, K. Kaehlcke, B. L. Marshall, A. Dorr, C. Hetzer-Egger, P. Henklein, R. Frye, M. W. McBurney, H. Hruby, M. Jung, E. Verdin, M. Ott, *PLoS Biol.* **2005**, *3*, e41.
[13] A. D. Napper, J. Hixon, T. McDonagh, K. Keavey, J. F. Pons, J. Barker, W. T. Yau, P. Amouzegh, A. Flegg, E. Hamelin, R. J. Thomas, M. Kates, S. Jones, M. A. Navia, J. O. Saunders, P. S. DiStefano, R. Curtis, *J. Med. Chem.* **2005**, *48*, 8045 – 8054.
[14] O. R. Bereshchenko, W. Gu, R. Dalla-Favera, *Nat. Genet.* **2002**, *32*, 606 – 613.
[15] B. Heltweg, T. Gatbonton, A. D. Schuler, J. Posakony, H. Li, S. Goehle, R. Kollipara, R. A. Depinho, Y. Gu, J. A. Simon, A. Bedalov, *Cancer Res.* **2006**, *66*, 4368 – 4377.
[16] K. T. Howitz, K. J. Bitterman, H. Y. Cohen, D. W. Lamming, S. Lavu, J. G. Wood, R. E. Zipkin, P. Chung, A. Kisielewski, L. L. Zhang, B. Scherer, D. A. Sinclair, *Nature* **2003**, *425*, 191 – 196.
[17] T. E. Voogd, E. L. Vansterkenburg, J. Wilting, L. H. Janssen, *Pharmacol. Rev.* **1993**, *45*, 177 – 203.
[18] M. U. Kassack, K. Braun, M. Ganso, H. Ullmann, P. Nickel, B. Boing, G. Muller, G. Lambrecht, *Eur. J. Med. Chem.* **2004**, *39*, 345 – 357.
[19] H. Ullmann, S. Meis, D. Hongwiset, C. Marzian, M. Wiese, P. Nickel, D. Communi, J. M. Boeynaems, C. Wolf, R. Hausmann, G. Schmalzing, M. U. Kassack, *J. Med. Chem.* **2005**, *48*, 7040 – 7048.
[20] K. A. Jacobson, S. Costanzi, M. Ohno, B. V. Joshi, P. Besada, B. Xu, S. Tchilibon, *Curr. Top. Med. Chem.* **2004**, *4*, 805 – 819.
[21] J. Trapp, A. Jochum, R. Meier, L. Saunders, B. Marshall, C. Kunick, E. Verdin, P. G. Goekjian, W. Sippl, M. Jung, *J. Med. Chem.* **2006**, *49*, 7307 – 7316.
[22] A. Schuetz, J. Min, T. Antoshenko, C. L. Wang, A. Allali-Hassani, A. Dong, P. Loppnau, M. Vedadi, A. Bochkarev, R. Sternglanz, A. N. Plotnikov, *Structure* **2007**, *15*, 377 – 389.
[23] B. Heltweg, F. Dequiedt, E. Verdin, M. Jung, *Anal. Biochem.* **2003**, *319*, 42 – 48.
[24] B. Heltweg, J. Trapp, M. Jung, *Methods* **2005**, *36*, 332 – 337.
[25] B. J. North, B. Schwer, N. Ahuja, B. Marshall, E. Verdin, *Methods* **2005**, *36*, 338 – 345.
[26] D. Cheng, N. Yadav, R. W. King, M. S. Swanson, E. J. Weinstein, M. T. Bedford, *J. Biol. Chem.* **2004**, *279*, 23892 – 23899.
[27] J. L. Avalos, K. M. Bever, C. Wolberger, *Mol. Cell* **2005**, *17*, 855 – 868.
[28] M. S. Finnin, J. R. Donigian, N. P. Pavletich, *Nat. Struct. Biol.* **2001**, *8*, 621 – 625.
[29] G. Jones, P. Willet, R. C. Glen, A. R. Leach, R. Taylor, *J. Mol. Biol.* **1997**, *267*, 727 – 748.
[30] P. Ferrara, H. Gohlke, D. J. Price, G. Klebe, C. L. Brooks III, *J. Med. Chem.* **2004**, *47*, 3032 – 3047.
[31] C. J. Lai, J. C. Wu, *Assay Drug Dev. Technol.* **2003**, *1*, 527 – 535.
[32] T. Antoshenko, J. R. Min, A. Schuetz, P. Loppnau, A. M. Edwards, C. H. Arrowsmith, A. Bochkarev, A. N. Plotnikov, *PDB codes: 2B4Y and 2FZQ*, **2007**, to be published: http://www.rcsb.org.
[33] M. Kassack, P. Nickel, *J. Chromatogr. B* **1996**, *686*, 275 – 284.
[34] Chemical Computing Group Inc., Montreal, Quebec, Canada, **2005**.
[35] H. Berman, K. Henrick, H. Nakamura, *Nat. Struct. Biol.* **2003**, *10*, 980.
[36] R. A. Laskowski, M. W. MacArthur, D. S. Moss, J. M. Thornton, *J. Appl. Crystallogr.* **1993**, *26*, 283 – 291.
[37] W. C. Still, A. Tempczyk, R. C. Hawley, T. Hendrickson, *J. Am. Chem. Soc.* **1990**, *112*, 6127 – 6129.
[38] GROMACS 3.2.1, University of Groningen (The Netherlands).
[39] L. A. Kelley, S. P. Gardner, M. J. Sutcliffe, *Protein Eng.* **1996**, *9*, 1063 – 1065.
[40] P. J. Goodford, *J. Med. Chem.* **1985**, *28*, 849 – 857.

Received: January 9, 2007
Revised: June 19, 2007
Published online on July 12, 2007

